ARTICLE

BIOTECHNOLOGY and BIOENGINEERING

Improved Recellularization of Ex Vivo Vascular Scaffolds using Directed Transport Gradients to Modulate ECM Remodeling

Zehra Tosun, Peter S. McFetridge

J. Crayton Pruitt Family Department of Biomedical Engineering, University of Florida, 1275 Center Drive, Biomedical Sciences Building, JG-56, Gainesville, Florida, 32611; telephone: +352 273 9325; fax: +352 272 9221; e-mail: pmcfetridge@bme.ufl.edu

ABSTRACT: The regeneration of functional, clinically viable, tissues from acellular ex vivo tissues has been problematic largely due to poor nutrient transport conditions that limit cell migration and integration. Compounding these issues are subcellular pore sizes that necessarily requires extracellular matrix (ECM) remodeling in order for cells to migrate and regenerate the tissue. The aim of the present work was to create a directed growth environment that allows cells to fully populate an ex vivo-derived vascular scaffold and maintain viability over extended periods. Three different culture conditions using single (one nutrient source) or dual perfusion bioreactor systems (two nutrients sources) were designed to assess the effect of pressure and nutrient gradients under either low (50/30 mmHg) or high (120/80) relative pressure conditions. Human myofibroblasts were seeded to the ablumenal periphery of an ex vivo-derived vascular scaffold using a collagen/hydrogel cell delivery system. After 30 days culture, total cell density was consistent between groups; however, significant variation was noted in cell distribution and construct mechanics as a result of differing perfusion conditions. The most aggressive transport gradient was developed by the single perfusion low-pressure circuits and resulted in a higher proportion of cells migrating across the scaffold toward the vessel lumen (nutrient source). These investigations illustrate the influence of directed nutrient gradients where precisely controlled perfusion conditions significantly affects cell migration, distribution and function, resulting in pronounced effects on construct mechanics during early remodeling events.

Biotechnol. Bioeng. 2013;xxx: xxx–xxx.

KEYWORDS: bioreactors; recellularization; umbilical vein

Correspondence to: P. S. McFetridge

Contract grant sponsor: National Institutes of Health NIH
Contract grant number: R01HL0882
Received 25 July 2012; Revision received 16 December 2012; Accepted 18 December 2012
Accepted manuscript online xx Month 2012;
Article first published online in Wiley Online Library (wileyonlinelibrary.com).
DOI 10.1002/bit.24934

Introduction

Occlusive vascular disease results in excessively high morbidity and mortality rates and is one of the most significant clinical issues in modern western societies (Coen et al., 2009; Schmedlen et al., 2003). While autologous vessels remain the gold standard for bypass surgery, they are limited by supply, and current alternatives for small diameter (<6 mm) applications have unacceptably high failure rates. Typically, implant failure is driven by poor biological functionality, where high resistance and low flow compound occlusive events (John et al., 2005; Wang et al., 2007). Early attempts aimed at developing non-thrombogenic, passive conduits met with limited success and efforts became focused on improving biological functionality. Weinberg and Bell were the first to pioneer this approach using collagen hydrogels seeded with smooth muscle cells, fibroblasts and endothelial cells to produce a completely biological blood vessel (Weinberg and Bell, 1986). Initial clinical forays to improve functionality lined non-degrading grafting materials with endothelial cells with the aim to minimize thrombotic and inflammatory responses (Zilla et al., 2007). The improved patency of these vessels shifted the attention of the scientific community towards maximizing biological functionality to allow adaptation to changing hemodynamic and metabolic conditions (Greenwald and Berry, 2000). As a result of their creative work, tissue engineering has become a compelling strategy to create small diameter blood vessels for reconstructive surgeries (Isenberg et al., 2006; Thomas et al., 2003; Wang et al., 2007).

While promising, engineering or de novo regeneration of a functional vascular intima and media within limited clinical time frames has been problematic (Barron et al., 2003; Mitchell and Niklason; Nerem, 2003; Nerem and Seliktar, 2001; Schmedlen et al., 2003) As such, creating a cell dense scaffold in a timely fashion is a crucial step towards recapitulating a muscular medial layer with vasoactive behavior and suitable mechanical properties. The initial step with all scaffold types is to seed cells that will ultimately function as vascular smooth muscle cells (vSMC) that are then required to migrate into the scaffold

and proliferate to create the smooth muscle layer (Chan-Park et al., 2009).

The concept behind the use of ex vivo vascular tissues as a decellularized scaffolding material is to preserve the essential extracellular matrix components that provide a more natural mechanical and chemical environment that maximizes the concept of guided tissue regeneration. However, cell infiltration is inhibited within ex vivo-derived scaffolds as seeded cells are limited to the scaffold periphery as subcellular pore sizes prevent passive cell dispersion into the scaffold. This poses a barrier for passive cell migration and results in nutrient deprivation in areas most distant to the nutrient source (Yazdani et al., 2009).

Used as a model system to assess early vascular remodeling events, our previous investigations have shown dual circuit perfusion bioreactors (lumen and ablumenal flow perfusion) provided a nutrient rich environment that promoted cell proliferation and matrix deposition (Tosun et al., 2011). However, with a culture period of 3 weeks, cell populations had migrated a maximum of approximately 150 μm from the seeded surface and as such remained concentrated at the graft periphery. The inhibition of cell migration is primarily due to mass-transfer limitations that impede cell function proportionally to the relative importance of the specific nutrient (Rouwkema et al., 2009; Shakeel et al., 2011). In addition, the biologically complex structure of the natural vein (HUV) has anisotropic porosity and diffusion characteristics that are difficult to predict. This is highlighted with the compact and closely aligned fibers of the basement membrane where diffusion of larger molecular weight molecules and is limited (Moore et al., 2012).

Investigations described herein aimed to enhance cellular migration by applying directed transport gradients to promote transmural migration and more uniformly populated constructs. Using perfusion bioreactors, lumen pressure (either 120/80 mmHg [high pressure] or 50/30 mmHg [low pressure]) was used to modulate transmural hydraulic conductivity, either with, or without, media in the ablumenal flow circuit. Our hypothesis was that cells seeded on the ablumenal surface would respond to the more aggressive chemotactic nutrient gradients (driven by lumenal pressure and nutrient availability), by displaying increased migration with improved distribution toward the nutrient source, rather than being limited to the scaffold periphery.

Materials and Methods

Experimental Methods

Human Umbilical Vein (HUV) Dissection

These investigations conform to the principles outlined in the Declaration of Helsinki for use of human tissue or subjects, and approved by the University of Florida Institutional Review Board (approval #64-2010). Human umbilical cords were collected from Shands Hospital (Gainesville, FL) within four hours of delivery. The HUV was dissected automatically as previously described (Abousleiman et al., 2008a,b; Daniel et al., 2005). Briefly, 100 mm segments were cut from the cord and a stainless steel mandrel (0.250″OD × 6″ Length) was inserted through the vein lumen. Cords were stored at −86°C in a styrofoam container to allow progressive freezing at the rate of 2.5°C/min. Using a computer numerical control (CNC) system on a mechanical lathe (MicroKinetics, Kennesaw, GA), a simple script was run to automate the dissection process resulting in consistent scaffold wall thickness of 750 μm.

Decellularization

After dissection, vessels were thawed at 5°C then removed from mandrels. Decellularization steps were conducted at room temperature and under continuous agitation at 100 rpm using an orbital shaker. HUV segments were decellularized by washing in a 1% sodium dodecyl sulfate (SDS) solution and agitated. After 24 h the solution was discarded and the scaffolds were rinsed in distilled water for 10 min, 20 min, 1 h, 6 h, 24 h with solutions replaced at each time point. Samples were then incubated for 3 h in a 70 U/mL DNase (Sigma–Aldrich Inc., St. Louis, MO) solution in phosphate buffered saline (PBS). A representative image of HUV prior to and after decellularization is shown in supplemental data 1.

Cell Culture

Human myofibroblasts were purchased from ATCC (CRL-2854; VA) and maintained with low glucose (2 g/L) Dulbecco's modified Eagle's medium (DMEM; Hyclone, Carlsbad, Calif), supplemented with 10% fetal bovine serum, 1% L-glutamine, and 1% penicillin streptomycin (Hyclone) with 5% CO_2 at 37°C.

Bioreactor Assembly and Cell Seeding

Bioreactor assembly, cell culture, preparation of hydrogels, and cell seeding have been previously described (McFetridge, 2005; McFetridge et al., 2007; Montoya and McFetridge, 2009; Tosun et al., 2011). Briefly, three bioreactor systems were connected in series with standard silicone tubing using scaffold was prepared from different placental origins. After assembly, the system was sterilized by perfusing with a 0.2% peracetic acid and 4% ethanol solution for 2 h. Samples were then rinsed in distilled water and pH balanced in PBS. Bioreactors (with constructs) were then incubated with complete growth medium overnight (at 37°C with 5% CO_2). Human myofibroblasts were dispersed within a type 1 collagen hydrogel (Devro Medical, San Jose, CA) and inoculated into the shell-side void of the bioreactor to polymerize. After polymerization, progressive gel contraction occured around the ablumenal surface of the HUV scaffold. Final seeded cell density was 1×10^6 cells/linear cm scaffold.

Perfusion Flow Profile Design

After gel polymerization, culture media was circulated through the lumenal flow circuit at a maximum flow rate

of 10 mL/min for 24 h to maintain hydrogel stability. From Day 2 to Day 10 the flow rate was progressively increased to reach a maximum of 120 mL/min with a pulse frequency of 3 Hz. No media directed through the ablumenal flow circuit during this period. The same initial flow conditioning profile was used in all bioreactor sets from seeding to Day 10 at which point the specific flow and pressure regimes were initiated, detailed in Figure 1. All culture was under standard conditions of 5% CO_2 at 37°C. Flow rates were maintained 120 mL/min with 3 Hz frequency for all conditions. For these investigations a time point of 30 days was chosen to evaluate remodeling that extended past the 20 days of previous work (Tosun et al., 2011). Acronyms and description of each bioreactor condition are listed below.

- DP-ACHp: Dual perfusion: Acellular control (no seeded cells/lumen pressure 120/80 mmHg).
- DP-Hp: Dual perfusion: Seeded, with complete media in both flow circuits (lumen pressure 80/120 mmHg).
- SP-Lp: Single perfusion: Seeded, with complete media only in the lumenal circuit (lumen pressure 30–50 mmHg).
- SP-Hp: Single perfusion: Seeded, with complete media only in the lumenal circuit (lumen pressure 80/120 mmHg).

Dual perfusion (DP) refers to media flowing through two independent circuits, in this case lumen and ablumenal flow. Single perfusion (SP) by comparison perfuses media in only one of the aforementioned circuits, see Figure 1C.

Analytical Methods

After the completion of each experimental group, HUV constructs were removed from the bioreactors. Samples (5 mm ringlets) from proximal, mid, and distal positions were analyzed to assess scaffold morphology, cell density, metabolic activity, cell distribution, and biomechanical properties, as follows.

Cell Density and Metabolic Activity

Cell density was calculated indirectly by quantifying total DNA using a dsDNA quantification assay (PicoGreen, Invitrogen, Grand Island, NY). Calibration curves were produced for known concentrations of cells and DNA that was then used to calculate the DNA concentration/cell. The metabolic activity of each construct ringlet was determined using the AlamarBlue (Invitrogen) assay. Samples were incubated with 2 mL of media supplemented with 10% (v/v) AlamarBlue (AB) reactant, at 37°C for 6 h to allow the reduction to occur. Absorbance was then measured at two wavelengths: λ1, 570 nm and λ2, 600 nm using a plate reader (Synergy 2, Bio-Tek, Winooski, VT). Data for metabolic

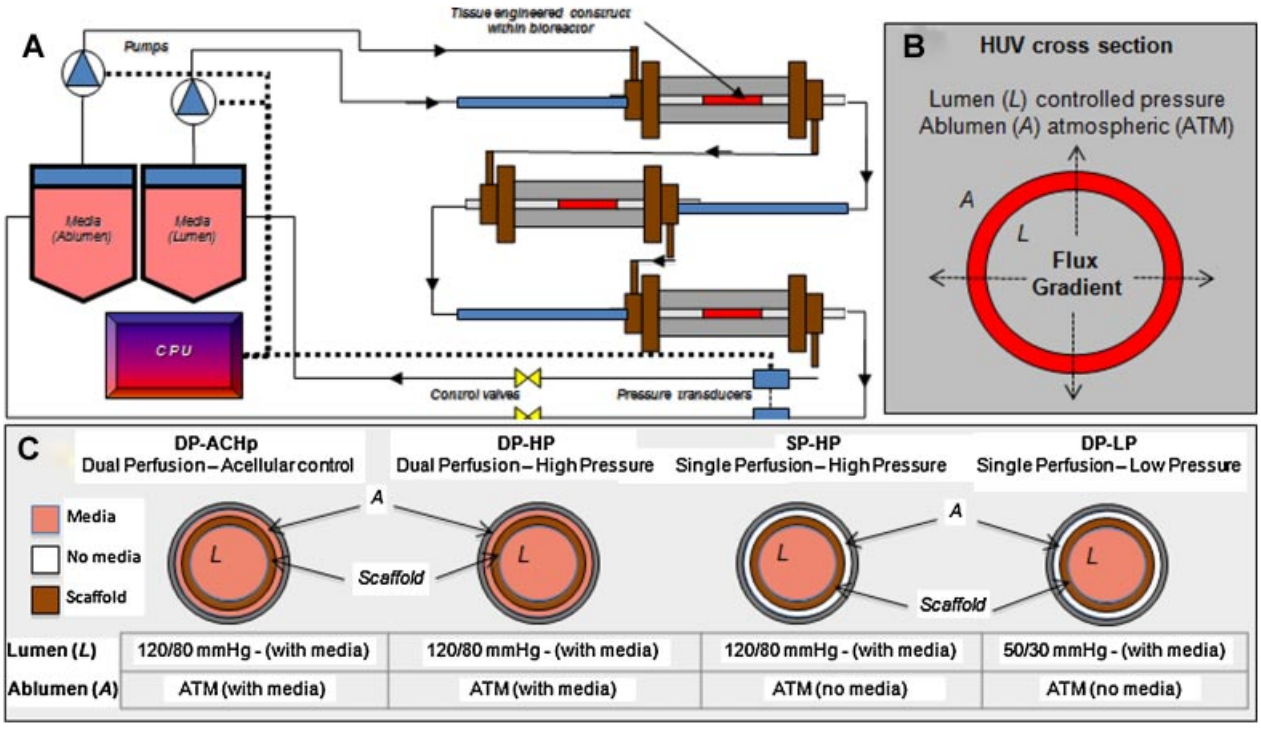

Figure 1. **A**: Dynamic cell culture process flow. Three bioreactors were connected in series as two independent flow circuits with discrete lumen and ablumen medium reservoirs, and rotary pumps. **B**: Schematic representation of the HUV scaffold cross section. **C**: Acronym, and the description of each bioreactor condition. Using perfusion bioreactors in panel (A), lumen pressure was used to develop a nutrient gradient, either with, or without, media in the ablumenal flow circuit, as seen in panel (B) and (C).

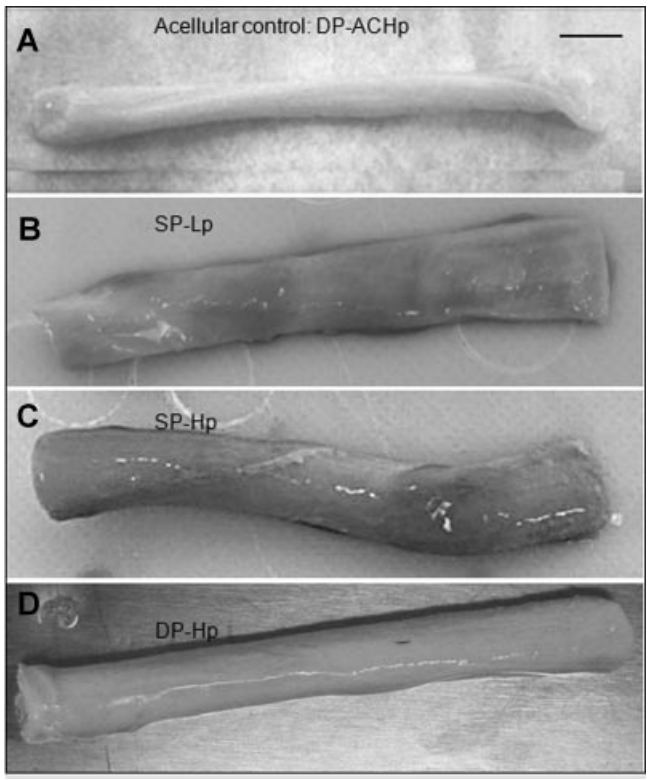

Figure 2. Representative images of vascular constructs. Acellular: DP-ACHp (**A**), SP-Lp (**B**) SP-HP (**C**), and DP-HP (**D**). The more substantial structure of the SP-Hp and DP-HP construct is shown comparative to the acellular material appears almost translucient and SP-Lp that has insufficient strength to maintain its tubular shape and after 30 days perfusion culture. Scale bars on left column images corresponds to 500 μm.

activity was combined with quantitative log cell density and expressed as the percentage of AB reduction per cell.

Histology

Sections were labeled with "SYTO RNA dye" as per manufacturer's instructions to quantify the gross distribution of RNA across the scaffold. "SYTO RNA dye" is a cell permeable nucleic acid stain, exhibiting a very weak signal when bound to DNA and a strong signal when bound to RNA (absorption/emission maxima ~490/530 nm) (Rhee and Bao, 2009). Samples were viewed using a Zeiss Axio Imager M2 microscope with Axiovision software release 4.6. The source images for RNA quantification were processed to measure pixel intensity of fluorescent areas by using a threshold command function script. Each of the images were then divided into three equally spaced sections representing lumen (1), mid-section (2) and ablumenal (3) zones.

Uniaxial Tensile Testing

Uniaxial tensile testing was conducted at room temperature using Instron 5542 single column testing rig with a 50 N capacity load cell (Instron 5542, Norwood, MA). Tissue specimens were loaded onto stainless steel L-shaped hooks (see Fig. 2) and were preloaded to a stress of 0.005 N at a rate of 5 mm/min and then elongated until failure, with force and extension recorded over time ($n = 9$). Tensile strength was obtained from the stress–strain data, corresponding to the maximum load that the samples withstood prior to rupture and normalized to the thickness of the layers. Young's modulus is a measure of materials stiffness (elasticity), and was calculated from the highest slope of the linear section of the stress–strain graph (Smith and Hashemi, 2010).

Burst Pressure

Using the ultimate tensile stress values (from the circumferential tensile testing) construct burst pressure was estimated using Laplace's relationship to derive the theoretical vessel burst pressure:

$$Pr = \sigma h \text{ (Laplace relationship)} \quad (1)$$

where P is the pressure; r, the radius; σ, the Cauchy stress; and h, the wall thickness (Stekelenburg et al., 2009).

Calculation of Scaffold Permeability

Permeability was assessed under low (50/30 mmHg) and high (120/80 mmHg) pressure profiles using Darcy's law. This equation expresses permeability as a function of the flow rate Q (m^3/s) and pressure drop ΔP across a matrix:

$$k = \frac{QL\mu}{A\Delta P} \text{ (Darcy's law)} \quad (2)$$

where A is the scaffold area (m^2), L is the matrix thickness (m), and μ is the dynamic solution viscosity (Pa s). Pressure (P) was monitored using a digital pressure gauge (model # EW-68332-06, Cole Parmer, Vernon Hills, IL) immediately downstream from the bioreactor.

Statistical Analysis

All data are presented as the mean ± standard deviation. Statistical significance ($P < 0.05$) was determined by multiple comparison test (Tukey test) using one way ANOVA. A table showing significance between conditions and assessment parameters is shown in Supplementary Data 2.

Results

Construct Morphology and Thickness

Gross morphology of cellular and acellular vascular constructs is shown in Figure 2. Construct thickness was measured in the proximal, mid and distal positions, with the initial HUV thickness (prior to hydrogel based seeding) being 0.75 mm. The total thickness of HUV and hydrogel composite (prior to gel contraction) was 6.0 mm, as presented in Figure 3. The overall thickness of constructs cultured using the single perfusion-high pressure system (SP-Hp) was 0.54 ± 0.43 mm, with acellular control scaffolds under dual perfusion conditions (DP-ACHp) 1.56 ± 0.41 mm, dual perfusion-high pressure (DP-Hp) at 1.02 ± 0.3 mm, and single perfusion low pressure (SP-Lp) 1.18 ± 0.45 mm, as seen in Figure 3.

Biomechanical Properties

Analysis of the constructs tensile properties displayed two distinct failure peaks, as shown in Figure 3. Observed fracture peaks were associated with an inner region consisting of the vessels' original medial layer, and the outer region composed of adventitial tissue that transition to the specialized glycosaminoglycan rich connective tissue of the Wharton's jelly.

After 30 days perfusion culture, the inner region of constructs exposed to the single perfusion higher pressure system (SP-Hp: 120/80 mmHg) to have significantly higher tensile strength of 734 ± 210 kPa relative to the low pressure system (SP-Lp: 50/30 mmHg) with 305 ± 62 kPa. Acellular controls (DP-ACHp) decreased from 550 ± 41 to 314 ± 35 kPa. Results for the outer region' tensile strength displayed a similar trend with the high pressure systems

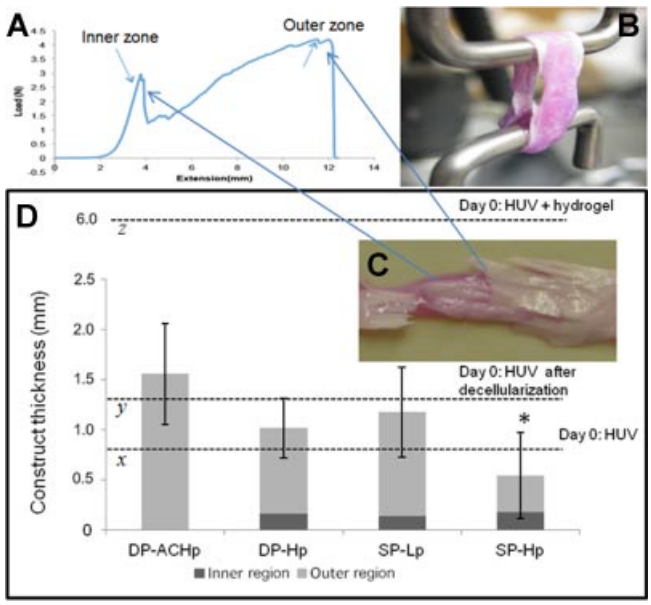

Figure 3. Representative circumferential tensile stress–strain relationship (**A**) of the cellular constructs, images of a cellular construct ringlet after failure (**B** and **C**) for the clarification of inner and outer zones. (**D**). Construct thickness. Thickness of the constructs of inner and outer zones, and cumulative thickness for all conditions after 30 days of perfusion culture. The initial average value for the wall thicknesses of HUV before (*x*) and after decellularization (*y*), and immediately after collagen gel seeding (*z*) are represented with dashed lines. *Significant difference in thickness between SP-HP, and DP-ACHP ($P < 0.005$).

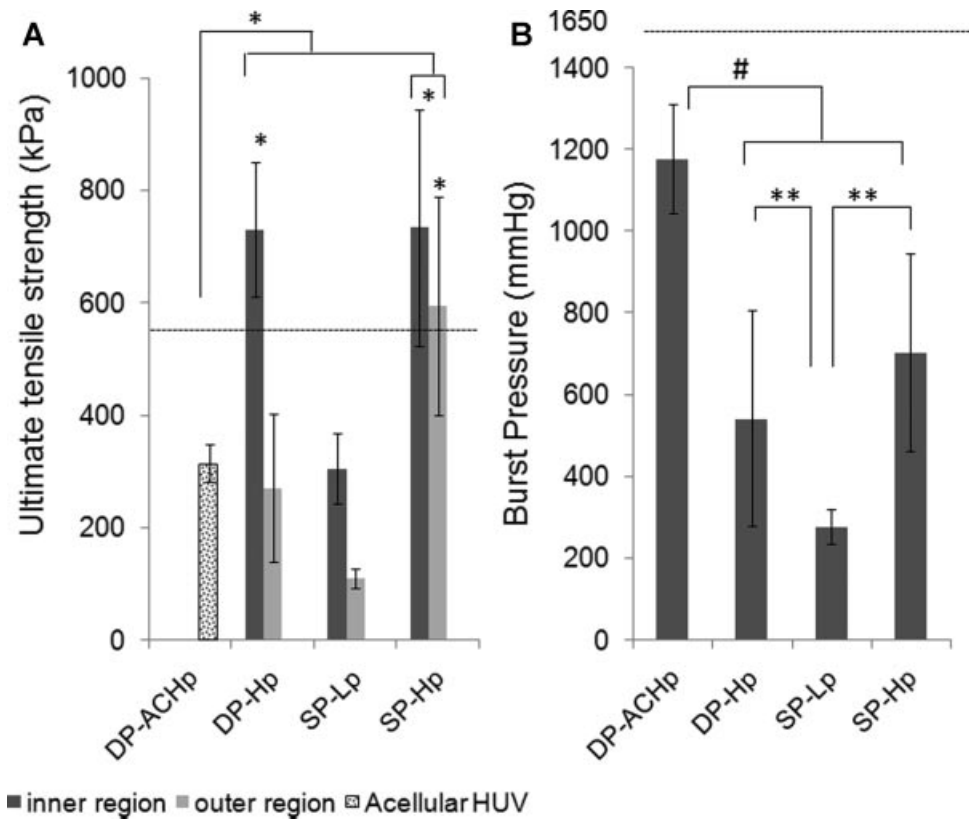

Figure 4. Tensile strength (TS) of inner and outer zone of the constructs (**A**). Calculated Burst pressure values derived from the Laplaces Law (**B**). Acellular controls at day = 0 is shown with a dashed line. *Significant higher UTS compared to acellular control set (DP-ACHp), and SP-LP ($P < 0.001$). **Burst pressure of SP-Hp significantly higher than SP-Lp ($P < 0.05$). #Burst pressure of DP-ACHP was statistically higher than all of the conditions (DP-Hp, and SP-Lp $P < 0.001$, SP-Hp $P < 0.05$), $n = 9$.

trending higher relative to controls or low pressure constructs, as shown in Figure 4A.

Burst pressure values calculated from Laplace equation are DP-Hp: 542 ± 263 mmHg, SP-Lp: 276 ± 42 mmHg, SP-Hp: 705 ± 242, and DP-ACHp: 1177 ± 135, as shown in Figure 4B. Young's modulus and % strain at max load values are presented in Figure 5. Young's modulus values show the dual perfusion high pressure construct to have significantly stiffer inner tissue regions compared to low pressure conditions, as follows: DP-Hp: $4{,}578 \pm 1{,}718$ kPa, SP-Lp: 920 ± 294, and SP-Hp: $4{,}078 \pm 2{,}442$. The outer region was shown to be more elastic with Young's modulus values significantly lower than the inner region; DP-Hp: 277 ± 122 kPa, and SP-Lp: 98 ± 35 kPa, SP-Hp: 396 ± 144 kPa. The Young's modulus values in the outer region of SP-Hp, and DP-Hp were similar, while SP-Lp had statistically lower values.

There was no statistical difference in the strain at maximum load values. The inner region failed first at approximately 50% strain; the outer region, which consisted of Wharton's jelly-hydrogel remodeled scaffold, failed at approximately 175% strain, which was similar to acellular HUV values.

Scaffold Cellularity

While SP-Hp constructs displayed higher average cell densities, both cell density and metabolic activitywere statistically similar between all groups, as shown in Figure 6 Cell density increased up to eight times the original seeding density of 1×10^6 cells/linear cm to terminal densities of $4.81 \pm 2.07 \times 10^6$ (DP-Hp), $4.27 \pm 1.84 \times 10^6$ (SP-Lp), and $8.12 \pm 4.80 \times 10^6$ cells/cm/linear (SP-Hp) scaffold.

Cell distribution

Fluorescence RNA labeling was used to localize cells within the scaffold and as an indirect method to assess cell viability. All images in Figure 7 are oriented with the constructs ablumen (seeded surface) on the right-hand side, and the lumen on the left. Figure 7A, D, and G (left column) displays representative images of constructs under standard fluorescent conditions to highlight the ECM structure and localize RNA labeled cells. Images in center panel (Fig. 7B, E, and H) were obtained using fluorescent thresholding to isolate RNA stained cells from background non-specific ECM binding. Each image of the vessel wall was divided into three equal

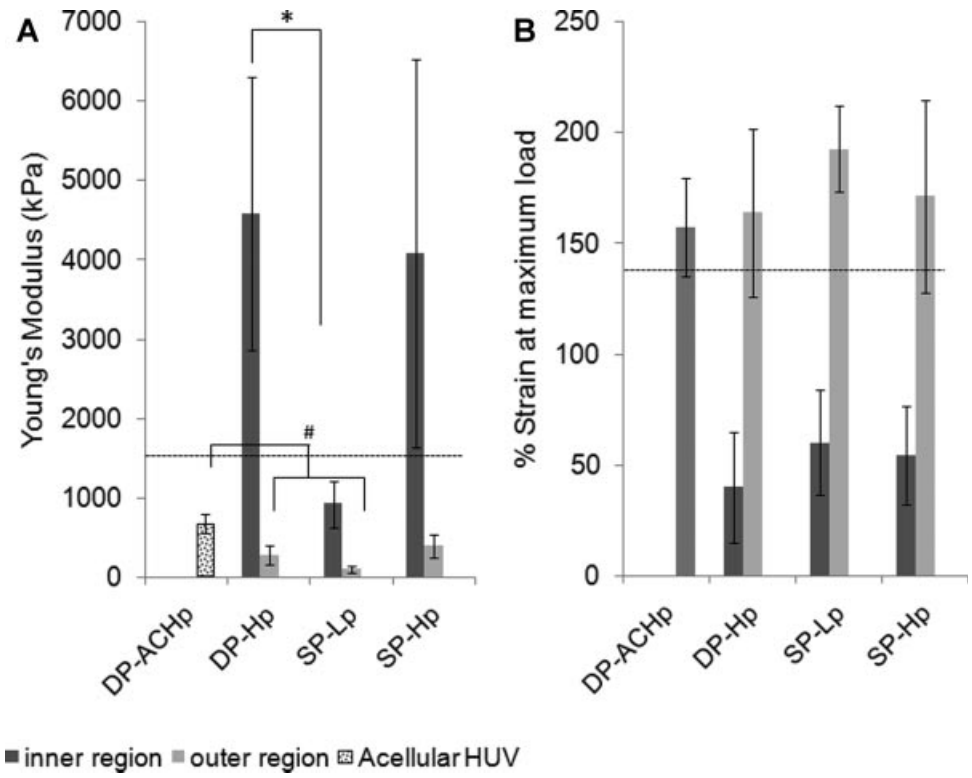

Figure 5. Comparison of Youngs modulus (**A**), and % strain at max load (**B**) of constructs after 30 days of culture. Acellular controls at day = 0 is shown with a dashed line. *Youngs modulus of inner zone DP-Hp significantly higher than values for the inner zone of SP-Lp but similar to SP-Hp inner zone, $P < 0.05$. #Youngs modulus of acellular control DP-ACHp set was higher than outer zone of DP-Hp ($P < 0.005$), and SP-Lp ($P < 0.001$) but similar to SP-Hp outer zone.

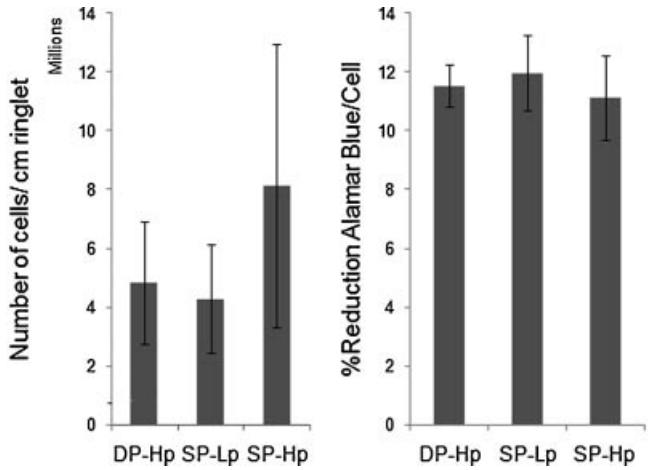

Figure 6. Cell density and metabolic activity. Cell density (above left) of cellular HUV constructs at Day 30. Cell seeding density is shown with a dashed line. Values indicate mean ± standard deviation. Metabolic Activity/cells (above right) of the vascular constructs with Alamar Blue dye. No statistical difference of metabolic activity/cell value was observed and values were consistent with our previous work.

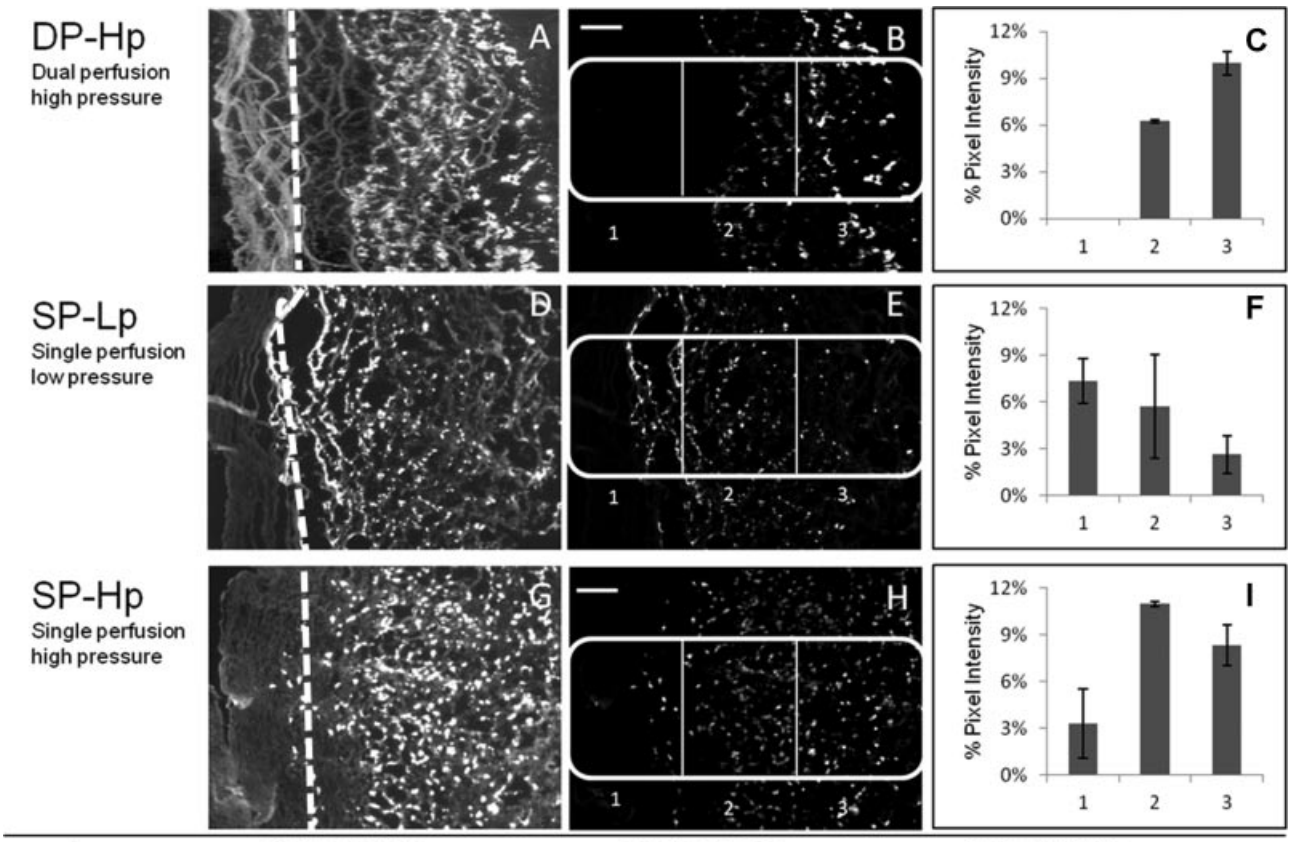

p value	DP-Hp/SP-Lp	DP-Hp/SP-Hp	SP-Lp/SP-Hp
Zone 1	0.002*	0.082	0.039*
Zone 2	0.939	0.052	0.035*
Zone 3	0*	0.237	0.002*

Figure 7. Fluorescence RNA labeling was used to localize cells within the scaffold and as an indirect method to assess cell viability (**A**, **D**, and **G**) Inner and outer regions displaying distinct mechanical properties are demarcated with a dotted line. For comparison of cell density within scaffold, each image was divided into sections (1–3) from lumen to ablumen (**B**, **E**, and **H**), and fluorescence pixel intensity (% pixels white) was measured for each region (**C**, **F**, and **I**). Scale bars (center panel images) correspond to 100 μm.

zones (1–3) to quantify cell distribution across the scaffold. Figure 7C, F, and I represents pixel intensity (% pixels white) derived from the fluorescently labeled RNA within each section and given as a percentage intensity value.

Across all perfusion systems, cells were shown to adhere, proliferate and migrate into the scaffold over the culture period, providing evidence for active remodeling. Constructs exposed to complete media on both surfaces under physiological pressure conditions (DP-Hp) displayed the least migration across the scaffold with cells significantly denser in zone 3 adjacent the seeded surface, with a reduced density in zone 2, and no cells detected within the more distant zone 1 which was adjacent to the lumen of the vessel (see Fig. 7A–C). Constructs cultured using single perfusion low pressure systems (SP-Lp) resulted in higher (relative) concentrations of cells in zones 1 and 2 with reduced densities adjacent to the seeded surface in zone 3 (see Fig. 7D–F). Single perfusion, high pressure systems (SP-Hp) resulted in similarly distributed RNA in the zone 2 zone 3, and lower concentrations in zone 1 (see, Fig. 7G–I). Comparison of leading edge of cell migration between conditions is presented in supplemental data 3.

Permeability

Scaffold permeability was calculated for each pressure, using a mean thickness value of 0.75 μm. The average permeability coefficients were $1.20 \pm 0.33 \times 10^{-12}$ m^2 at low pressure (50/30 mmHg), and $2.23 \pm 0.4 \times 10^{-12}$ m^2 at high pressure (120/80 mmHg). High pressure resulted in a significantly higher permeability coefficient relative to low pressure systems ($P = 0.026$).

Discussion

Creating a cell dense engineered construct has been a significant obstacle for decellularized tissue-based scaffolds as seeded cells are typically limited to the outer most surfaces

due to low porosity and nutrient depletion. This results in the formation of a cellular capsule around the construct, that further impedes migration as a progressively more hypoxic and nutrient deprived environment is created within the scaffold. Due to clinical requirements for rapid graft development, improving the rate at which scaffolds are repopulated is a key research objective. This is particularly important with bypass surgery where the time frame of development needs to be days, not weeks or months (He et al., 2010; Neff et al., 2011; Yazdani et al., 2009).

Currently, engineered vascular tissues require an extended culture period lasting upward of 2 months, often significantly longer to create vessels with biomechanical properties similar to native vessels (Dahl et al., 2011; McAllister et al., 2008, 2009). In order to improve SMC construct density and remodeling a number of different approaches have been taken, for example pulsatile radial stress through a distensible mandrel (Niklason et al., 1999; Seliktar et al., 2001; Stegemann and Nerem, 2003). In these systems over the first few weeks of culture the nutrient source is unidirectional from the ablumenal surface as no nutrients are available from the lumen. As such the delivery of nutrients to cells seeded on the ablumen is reliant on passive diffusion processes rather than pressure driven gradients. Isenberg et al. initially used a similar perfusion approach with fibrin-based scaffolds (Isenberg and Tranquillo, 2003); however, more recently they have focused on perfusion conditions that direct the bulk flow of cell culture media through lumen, with indirect transmural flow through the porous construct wall (Syedain et al., 2011). Constructs were grown under static conditions for 7 days, after which media was perfused through the lumen. After 9 weeks of culture, construct were extensively remodeled with burst pressures ranging from 1,400 to 1,600 mmHg and compliance comparable to native arteries (Syedain et al., 2011). Unlike synthetic scaffolds with controllable porosity and permeability, scaffolds derived from ex vivo-derived materials often have subcellular pore sizes with less favorable transport conditions. In addition to transport limitations, migration in these scaffolds is often limited due to the requirement of active cellular processes to digest the ECM in order to migrate. While several groups have demonstrated that vascular SMC's can grow, infiltrate and remodel up to 150–200 μm from the seeded surface in ex vivo materials, creating fully cell dense constructs has yet to be achieved (Dahan et al., 2012; Heine et al., 2011; McFetridge et al., 2007; Neff et al., 2011; Tosun et al., 2011; Yazdani et al., 2009).

The primary objective of this work was to assess key parameters that influence cell migration in order to design systems that improve cellular infiltration and reduce the in vitro culture phase of construct development. This is particularly important with scaffolds derived from natural tissues where pore size is subcellular limiting cell seeding and adhesion to the scaffold periphery.

Bioreactors with discrete shell and tube-side flow perfusion are designed to take advantage of generated pressure differentials encouraging controlled nutrient and gas transfer. Such perfusion systems create a significant driving force for nutrients across the scaffold wall. We therefore hypothesized that by controlling gradient conditions we could modulate cell migration and distribution within a limited nutrient environment. A controlled nutrient gradient was generated using either single or dual perfusion circuits, under low (50/30 mmHg) or high (120/80 mmHg) pulsed pressure profiles to assess the effects of nutrient gradients. The high pressure profile was chosen to emulate physiological conditions, while the lower values were chosen to create a more aggressive nutrient gradient as a function of reduced hydraulic conductivity.

Results show that between each of the perfusion conditions, gross cellularity was constant, but distinct differences were seen in cell distribution that was attributed to the characteristics of each perfusion condition. Constructs cultured under dual perfusion at high relative pressure (DP-Hp: 120/80 mmHg) displayed higher concentrations of cells located in the mid to outer layers of the scaffold, adjacent to the seeded surface. As cell density increased and progressively reduced the availability of nutrients from the ablumenal flow circuit, the nutrient source from the lumen began to play a more dominant role. As such, cell migration toward the lumen was initially slower due to sufficient nutrient availability from the ablumen, but as nutrients became limited, cells migrated toward the nutrient source from the lumen. At this point cells began to migrate and populate the mid region of the graft. These conditions are similar to those described by Yazdani et al. and McFetridge et al. also showing cells limited to the scaffold periphery.

Conversely, the low pressure single perfusion circuit (SP-Lp: 50/30 mmHg) created a more aggressive nutrient gradient due to media perfused through the lumen only and a reduced transmural flow relative to the higher pressure systems. The aggressive nutrient gradient became progressively more exaggerated as cell density increased resulting in cells behind the leading migration edge (closer to nutrient source) receiving less nutrients and a stronger chemotactic driving force toward the lumen. By the end of the 30-day culture period, these conditions resulted in the highest average densities toward the lumen interface (zone 1) and the lowest on the seeded surface (zone 3). By increasing the lumenal pressure to 120/80 mmHg (SP-Hp: 120/80 mmHg), cell migration was reduced. Under these conditions hydraulic conductivity increased due to the increased pressure drop resulting in an increase in transmural nutrient supply. This delivered higher concentration of nutrients to areas more distant from the lumen. This effectively reduced the chemotactic driving forces as metabolic demands were met. These data clearly show the importance of hydraulic permeability as a significant driving force in cell migration when nutrients are limited and consumption changes due to increasing cell densities.

While the total cell density in each test group was similar, significant differences in cell distribution and construct mechanics were shown. Single perfusion circuits at high pressure (SP-Hp: 120/80 mmHg) displayed significantly

higher outer zone tensile strength (TS) relative to all other seeded conditions. Conversely, the single perfusion system with low pressure (SP-Lp) resulted with the lowest Young's modulus and tensile strength values. From this data the main structural component of the scaffold (at least initially) was the inner zone 1, the zone comprising the vessels intimal and medial layers The two conditions that had the highest TS in the inner region (DP-Hp and SP-Hp) had the least cell populations present. This would imply that the initial migration processes, as cells digest the ECM, has resulted in mechanically weaker, lower modulus material. As seen in zone 3, where cells were seeded, higher pressure with increased cyclic strain (SP-Hp) resulted in the highest tensile strength, this is indicative of enhanced remodeling leading to improved mechanical properties.

These differences in mechanical performance were directly related to observed differences in cell function between groups. Increasing the cyclic pressure from 50/30 to 120/80 mmHg increased circumferential compliance, a stimulatory mechanical effect that has been shown to enhance remodeling activity by upregulation of ECM expression and deposition (Birukov et al., 1995; Wilson et al., 1993). In addition the increased pressure results in improved transmural delivery of nutrients to cells (from the lumen) relative to the lower pressure systems that typically inhibit growth. These remodeling changes are particularly important in vascular tissues because any potential for scaffold weakening during early remodeling may have catastrophic consequences, and as such a balance between ECM synthesis and degradation is an important factor. These interactions are clearly complex and multifactorial and as such require further investigation to define key influencing parameters.

These investigations describe controlled perfusion conditions that aim to rapidly repopulate and uniformly distribute cells within an ex vivo tissue scaffold We have focused on the effects of variable transport conditions rather than detailing conditions due to the clinical importance of recellularizing these materials and the complexity of the anisotropic material. While the in vivo environment is clearly more complex, the conditions generated with the SP-Hp circuit would be similar to those experienced clinically as a graft when implanted in the arterial vasculature. As such the perfusion systems described herein aim to emulate in vivo implant conditions where nutrients are only provided through the lumenal blood supply (100%), verses the ablumenal circuit that is without a direct nutrient supply (effectively 0%). These model systems provide a more detailed perspective of graft remodeling both in vitro and in vivo, where diffusion limits nutrient transfer and thus graft performance. Further, from a tissue engineering perspective, these investigations have shown that by modulating perfusion culture conditions, the density and the distribution of the viable cells can be regulated to improve construct mechanics and graft maturation. Future studies will focus on enhancing functional characteristics to obtain a vasoactive construct with a continuous endothelial cell layer.

References

Abousleiman RI, Reyes Y, McFetridge P, Sikavitsas V. 2008a. The human umbilical vein: A novel scaffold for musculoskeletal soft tissue regeneration. Artif Organs 32(9):735–741.

Abousleiman RI, Reyes Y, McFetridge P, Sikavitsas V. 2008b. Tendon tissue engineering using cell-seeded umbilical veins cultured in a mechanical stimulator. Tissue Eng Part A 15(4):787–795.

Barron V, Lyons E, Stenson-Cox C, McHugh PE, Pandit A. 2003. Bioreactors for cardiovascular cell and tissue growth: A review. Ann Biomed Eng 31 (9):1017–1030.

Birukov KG, Shirinsky VP, Stepanova OV, Tkachuk VA, Hahn AWA, Resink TJ, Smirnov VN. 1995. Stretch affects phenotype and proliferation of vascular smooth muscle cells. Mol Cell Biochem 144(2):131–139.

Chan-Park MB, Shen JY, Cao Y, Xiong Y, Liu Y, Rayatpisheh S, Kang GC-W, Greisler HP. 2009. Biomimetic control of vascular smooth muscle cell morphology and phenotype for functional tissue-engineered small-diameter blood vessels. J Biomed Mater Res Part A 88A(4):1104–1121.

Coen DAS, Denis C, Christopher D, Curt D, Jan Willem E, Marc L, Daniel S. 2009. Peripheral arterial disease: A growing problem for the internist. Eur J Intern Med 20(2):132–138.

Dahan N, Zarbiv G, Sarig U, Karram T, Hoffman A, Machluf M. 2012. Porcine small diameter arterial extracellular matrix supports endothelium formation and media remodeling forming a promising vascular engineered biograft. Tissue Eng Part A 18(3–4):411–422.

Dahl SLM, Kypson AP, Lawson JH, Blum JL, Strader JT, Li Y, Manson RJ, Tente WE, DiBernardo L, Hensley MT. 2011. Readily available tissue-engineered vascular grafts. Sci Transl Med 3(68):68ra9.

Daniel J, Abe K, McFetridge PS. 2005. Development of the human umbilical vein scaffold for cardiovascular tissue engineering applications. ASAIO J 51(3):252–261.

Greenwald SE, Berry CL. 2000. Improving vascular grafts: The importance of mechanical and haemodynamic properties. J Pathol 190(3):292–299.

He W, Nieponice A, Soletti L, Hong Y, Gharaibeh B, Crisan M, Usas A, Peault B, Huard J, Wagner WR, et al. 2010. Pericyte-based human tissue engineered vascular grafts. Biomaterials 31(32):8235–8244.

Heine J, Schmiedl A, Cebotari S, Mertsching H, Karck M, Haverich A, Kallenbach K. 2011. Preclinical assessment of a tissue-engineered vasomotive human small-calibered vessel based on a decellularized xenogenic matrix: Histological and functional characterization. Tissue Eng Part A 17(9–10):1253–1261.

Isenberg BC, Tranquillo RT. 2003. Long-term cyclic distention enhances the mechanical properties of collagen-based media-equivalents. Ann Biomed Eng 31(8):937–949.

Isenberg BC, Williams C, Tranquillo RT. 2006. Small-diameter artificial arteries engineered in vitro. Circ Res 98(1):25–35.

John DK, Christos DL, Christopher B, Bauer ES. 2005. Artificial blood vessel: The Holy Grail of peripheral vascular surgery. J Vasc Surg 41(2):349–354.

McAllister TN, Dusserre N, Maruszewski M, L'Heureux N. 2008. Cell-based therapeutics from an economic perspective: Primed for a commercial success or a research sinkhole? Regener Med 3(6):925–937.

McAllister TN, Maruszewski M, Garrido SA, Wystrychowski W, Dusserre N, Marini A, Zagalski K, Fiorillo A, Avila H, Manglano X, et al. 2009. Effectiveness of haemodialysis access with an autologous tissue-engineered vascular graft: A multicentre cohort study. The Lancet 373 (9673):1440–1446.

McFetridge PS, Chaudhuri JB. 2005. Design of vascular graft bioreactors: Bioreactors for tissue engineering. Principles, Design and Operation. Netherlands: Springer. p 269–283. DOI: 10.1007/1-4020-3741-4_12

McFetridge PS, Abe K, Horrocks M, Chaudhuri JB. 2007. Vascular tissue engineering: Bioreactor design considerations for extended culture of primary human vascular smooth muscle cells. ASAIO J 53(5):623–630.

Mitchell SL, Niklason LE. 2003. Requirements for growing tissue-engineered vascular grafts. Cardiovasc Pathol 12(2):59–64.

Montoya CV, McFetridge PS. 2009. Preparation of ex vivo—Based biomaterials using convective flow decellularization. Tissue Eng Part C Methods 15(2):191–200.

Moore M, Sarntinoranont M, McFetridge P. 2012. Mass transfer trends occurring in engineered ex vivo tissue scaffolds. J Biomed Mater Res Part A 100A(8):2194–2203.
Neff LP, Tillman BW, Yazdani SK, Machingal MA, Yoo JJ, Soker S, Bernish BW, Geary RL, Christ GJ. 2011. Vascular smooth muscle enhances functionality of tissue-engineered blood vessels in vivo. J Vasc Surg 53 (2):426–434.
Nerem RM. 2003. Role of mechanics in vascular tissue engineering. Biorheology 40(1–3):281–287.
Nerem RM, Seliktar D. 2001. Vascular tissue engineering. Ann Rev Biomed Eng 3(1):225–243.
Niklason LE, Gao J, Abbott WM, Hirschi KK, Houser S, Marini R, Langer R. 1999. Functional arteries grown in vitro. Science 284(5413):489–493.
Rhee WJ, Bao G. 2009. Simultaneous detection of mRNA and protein stem cell markers in live cells. BMC Biotechnol 9(1):30.
Rouwkema J, Koopman BFJM, Van Blitterswijk CA, Dhert WJA, Malda J. 2009. Supply of nutrients to cells in engineered tissues. Biotechnol Gen Eng Rev 26(1):163–177.
Schmedlen RH, Elbjeirami WM, Gobin AS, West JL. 2003. Tissue engineered small-diameter vascular grafts. Clin Plast Surg 30(4):507–517.
Seliktar D, Nerem R, Galis Z. 2001. The role of matrix metalloproteinase-2 in the remodeling of cell-seeded vascular constructs subjected to cyclic strain. Ann Biomed Eng 29(11):923–934.
Shakeel M, Matthews PC, Graham RS, Waters SL. 2011. A continuum model of cell proliferation and nutrient transport in a perfusion bioreactor. Math Med Biol 30(1):21–44.
Smith WF, Hashemi J. 2010. Foundations of materials science and engineering, Vol. xviii, Dubuque, IA: McGraw-Hill. 1068 pp.
Stegemann JP, Nerem RM. 2003. Phenotype modulation in vascular tissue engineering using biochemical and mechanical stimulation. Ann Biomed Eng 31(4):391–402.
Stekelenburg M, Rutten MCM, Snoeckx LHEH, Baaijens FPT. 2009. Dynamic straining combined with fibrin gel cell seeding improves strength of tissue-engineered small-diameter vascular grafts. Tissue Eng Part A 15(5):1081–1089.
Syedain ZH, Meier LA, Bjork JW, Lee A, Tranquillo RT. 2011. Implantable arterial grafts from human fibroblasts and fibrin using a multi-graft pulsed flow-stretch bioreactor with noninvasive strength monitoring. Biomaterials 32(3):714–722.
Thomas AC, Campbell GR, Campbell JH. 2003. Advances in vascular tissue engineering. Cardiovasc Pathol 12(5):271–276.
Tosun Z, Villegas-Montoya C, McFetridge PS. 2011. The influence of early-phase remodeling events on the biomechanical properties of engineered vascular tissues. J Vasc Surg 54(5):1451–1460.
Wang X, Lin P, Yao Q, Chen C. 2007. Development of small-diameter vascular grafts. World J Surg 31(4):682–689.
Weinberg C, Bell E. 1986. A blood vessel model constructed from collagen and cultured vascular cells. Science 231(4736):397–400.
Wilson E, Mai Q, Sudhir K, Weiss RH, Ives HE. 1993. Mechanical strain induces growth of vascular smooth muscle cells via autocrine action of PDGF. J Cell Biol 123(3):741–747.
Yazdani SK, Watts B, Machingal M, Jarajapu YP, Van Dyke ME, Christ GJ. 2009. Smooth muscle cell seeding of decellularized scaffolds: the importance of bioreactor preconditioning to development of a more native architecture for tissue-engineered blood vessels. Tissue Eng Part A 15(4):827–840.
Zilla P, Bezuidenhout D, Human P. 2007. Prosthetic vascular grafts: Wrong models, wrong questions and no healing. Biomaterials 28(34):5009–5027.

Supporting Information

Additional supporting information may be found in the online version of this article at the pulisher's web-site.